

# Comparison of performance of partial prestressed beam-column subassemblages made of reactive powder concrete and normal concrete materials using finite element models

S A Nurjannah\*, B Budiono, I Imran and S Sugiri

Graduate Program of Civil Engineering, Faculty of Civil and Environmental Engineering, Institut Teknologi Bandung  
Jl. Ganesha No. 10, Bandung, Indonesia

\*Corresponding author: sanurjannah@gmail.com

**Abstract.** Research on concrete material continues in several countries and had produced a concrete type of Ultra High Performance Concrete (UHPC) which has a better compressive strength, tensile strength, flexural strength, modulus of elasticity, and durability than normal concrete (NC) namely Reactive Powder Concrete (RPC). Researches on structures using RPC material showed that the RPC structures had a better performance than the NC structures in resisting gravity and lateral cyclic loads. In this study, an experiment was conducted to apply combination of constant axial and lateral cyclic loads to a prototype of RPC interior partial prestressed beam-column subassemblage (prototype of BCS-RPC) with a value of Partial Prestressed Ratio (PPR) of 31.72% on the beam. The test results were compared with finite element model of beam-column subassemblage made of RPC by PPR of 31.72% (BCS-RPC-31.72). Furthermore, there was BCS-RPC modeling with PPR of 21.39% (BCS-RPC-21.39) and beam-column subassemblages made of NC materials modeling with a value of PPR at 21.09% (BCS-NC-21.09) and 32.02% (BCS-NC-32.02). The purpose of this study was to determine the performance of the BCS-RPC models compared to the performance of the BCS-NC models with PPR values below and above 25%, which is the maximum limit of permitted PPR. The results showed that all models of BCS-RPC had a better performance than all models of BCS-NC and the BCS-RPC model with PPR above 25% still behaved ductile and was able to dissipate energy well.

## Introduction

Research on Ultra High Performance Concrete (UHPC) has produced a high-performance concrete in compressive strength, tensile strength, flexural strength, modulus of elasticity, and durability namely Reactive Powder Concrete (RPC). RPC consists of micro-sized material composed of silica sand, silica flour, silica fume, and superplasticizer, that leads it has a compact behavior better than Normal Concrete (NC). To increase the compressive strength since early age and accelerate the hydration process, RPC was treated in a steamed room or placed in hot water under temperature of 90° Celsius for three days. In an ideal condition of laboratory, the compressive strength of 120-230 MPa was achieved by RPC cylinders, while the RPC cylinders restrained by steel sleeves achieved the compressive strength of 490-680 MPa [1].

## Literature Review

The use of open frame structures reinforced by partial prestressed strands are commonly used to reduce the dimensions of the structural elements and expand the space. The partial prestressed structures are



more ductile and able to dissipate earthquake energy better than fully prestressed structures [2]. Prestressed strands in the plastic hinges are placed unbondedly and the maximum limit of Partial Prestressed Ratio (PPR) is 25% to ensure the structure remains ductile under earthquake loads [3].

The results of research on RPC material that had been done by Richard and Cheyrezy were developed by Gowripalan, et. al. [4] and Graybeal [5] by changing the composition of the material forming the RPC. The results showed that the RPC composed by different material composition had a higher performance than NC and had a compressive strength that was relatively similar to RPC had been created by Richard and Cheyrezy. Menefy [6] did research of bending load on the RPC beams used RPC mixture composition that developed by Gowripalan and produced cylinder compressive strength of 125-194 MPa. The RPC beams showed better performance than NC beams in the experiments. In this study, the composition of the RPC referred to a composition that had been developed by Naibaho, et al. [7]. There was an additional volume fraction of polypropylene fiber up to 0.08%.

The beam-column subassembly structures were analyzed using discrete element models of three-dimensional finite element. Finite element modeling of reinforced concrete was done by setting concrete, mild steels and prestressed strands as separate discrete elements. Finite element analysis performed by ANSYS program. Concrete elements were modeled as SOLID65 elements which are three dimensional elements and has eight nodals. Each node has three translational degrees of freedom in the direction of X, Y, and Z axes as shown in figure 1. SOLID65 was modeled as element that fractured by tensile stress, crushing due to compressive stress, plastic deformation, and creep. Modeling of longitudinal mild steels, transversal mild steels, and longitudinal prestressed strands elements used LINK8 elements. The forces acting on the elements were axial forces on the ends of the elements as shown in figure 2.

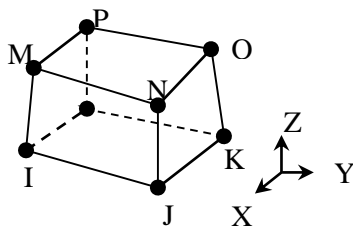


**Figure 1.** Test Set Up of SBC-RPC Prototype.

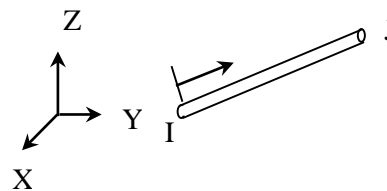


**Figure 2.** Cyclic Lateral Loading History Based on Deflection Control.

In the structure field, the equilibrium equation for the linear system is expressed as:

$$[K]\{u\} = \{F^a\} \quad (1)$$

where:

$[K]$  : structure stiffness matrix  
 $\{u\}$  : degrees of freedom vector  
 $\{F^a\}$  : load vector

In the nonlinear case, equation (1) could not be directly used. The iteration process was required to obtain a solution of the equation. In the ANSYS program, there were several methods that can be used to obtain convergent solutions. One of them was the Newton-Raphson method. This method is an iterative process in solving nonlinear equations. In this study, the method chosen for the ANSYS program was Full Newton-Raphson method, where the stiffness matrix was updated in each iteration as expressed in equation (2) and equation (3).

$$[K_i^T]\{\Delta u_i\} = \{F^a\} - \{F_i^{nr}\} \quad (2)$$

$$\{u_{i+1}\} = \{u_i\} + \{\Delta u_i\} \tag{3}$$

where:

- $[K_i^T]$  : structure stiffness matrix
- $\{u_i\}$  : degrees of freedom vector
- $\{F_i^{nr}\}$  : load vector

**Prototype and Experiment Methods**

In experimental studies, there was a prototype of interior Beam-Column Subassemblage made of RPC (BCS-RPC) with Partial Prestressed Ratio (PPR) of 31.72% on the beam. This prototype were part of five prototypes that used for experiments on the influence of PPR variations to the beam-column subassemblages hysteretic behavior. Details of dimension and reinforcement of interior SBC-RPC prototype with PPR of 31.72% is shown in figure 3. The test set up is shown in figure 4. The prototype resisted a combination of a constant axial load of  $0.1 f_c' A_g$  at the top end of the column and lateral cyclic load at a distance of 350 mm from the upper end of the column based on deflection control [8] as shown in figure 5. The experiment was conducted in the Laboratory of Structure and Building Construction, Research and Development of Housing and Settlement Center, Ministry of Public Works, Indonesia.

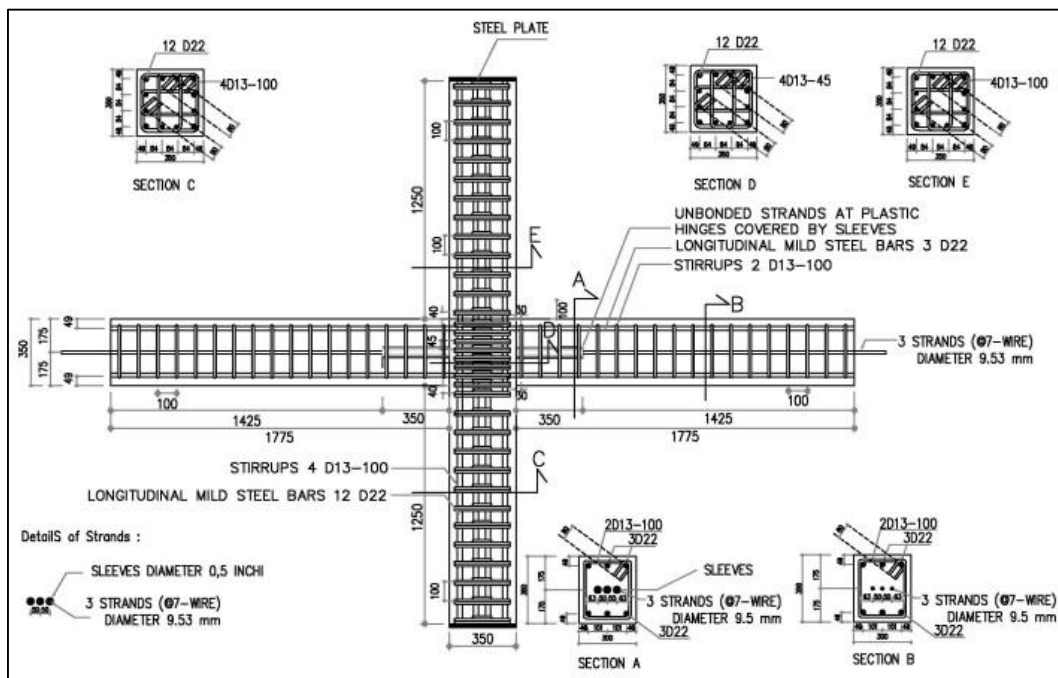


**Figure 3.** Details of Dimensions and Reinforcements of SBC-RPC Prototype.

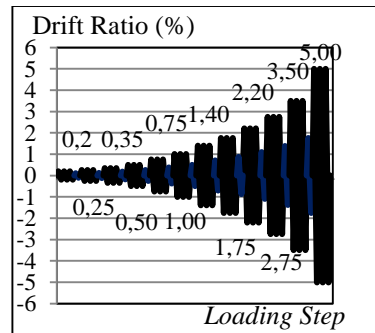
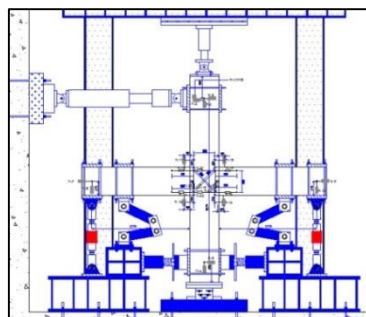


**Figure 4.** Experiment Set Up of SBC-RPC Prototype.**Figure 5.** Cyclic Lateral Loading History Based on Deflection Control.**Modeling of Beam Column Subassemblages by Finite Element Methods**

The beam-column subassemblage models were created by a nonlinear finite element program with varied values of PPR below and above 25%, while the concrete material structure was RPC and NC. PPR by 25% is the maximum value allowed as it had been presented in section 2. In the area of plastic hinges, the prestressed strands were placed unbondedly. The program input were the dimensions and details of the structure, as well as the stress-strain curves of each material that were parts of the structural models. The average compressive strength of RPC at 28 days for the program input was based on material experiments which will be elaborated in section 5. The NC compressive strength was set of 45 MPa. With the value of the NC compressive strength, the NC tensile strength and modulus of elasticity can be estimated using the following equations:

$$f_t = 0,62 \sqrt{f'_c} \text{ (T Class)} \quad (4)$$

$$E_c = 4700 \sqrt{f'_c} \quad (5)$$

where:

$f'_c$  : compressive strength of concrete (MPa)

$f_t$  : tensile strength of concrete (MPa)

$E_c$  : modulus of elasticity of concrete (MPa)

Thus, the values of tensile strength and modulus of elasticity of NC was 4.16 MPa and 31528 MPa, respectively. In the modeling, there were PPR and beam nominal moment variation as shown in table 1.

**Table 1.** Partial Prestressed Ratio and Nominal Moment of BCS-RPC and BCS-NC Models.

Strand	Strand Area	Concrete Type	Partial Prestressed Ratio	Model Code	Beam Nominal Moment
$A_p$	$A_p$		PPR		$M_n \text{ Beam}$
(mm <sup>2</sup> )	(mm <sup>2</sup> )		(%)		(kN.m)
1D12.7	98.71	RPC	21.39	BCS-RPC-21.39	140.19
3D9.5	164.52	RPC	31.72	BCS-RPC-31.72	154.87
2D9.5	109.68	NC	21.09	BCS-NC-21.09	152.39
2D12.7	197.42	NC	32.02	BCS-NC-32.02	171.22

**Results and Analysis**

In this study, there were material experiments, structure experiment of the BCS-RPC prototype with PPR of 31.72% (prototype BCS-RPC-31.72), and structure modeling used finite element method program. The material experiments results were used as input of BCS-RPC-31.72 modeling. Then, the hysteretic curve of the modeling result was compared with one of the structure experiment result of BCS-RPC-31.72 prototype. The hysteretic curve of model that behaved relatively close to the result of the experiment became a reference of BCS-RPC model with PPR of 21.39% (BCS-RPC-21.39) and BCS-NC models with PPR of 21.09% (BCS-NC-21.09) and 32.02% (BCS-NC-32.02).

*1.1. Testing Results of Reactive Powder Concrete Mixture Composition*

The compressive tests on cylindrical RPC samples were conducted at the age of 4, 7, 14 and 28 days. The first test was conducted at the age of four days because the samples were steamed for three days

before. At the age of 42 days, the compressive strength tests were conducted because there was a lateral cyclic loading experiment of the prototype BCS-RPC-31.72. The test results are displayed in the form of curves in figure 6. The figure shows that the compressive strength ( $f_c$ ) of concrete was relatively the same since the age ( $t$ ) of 4 days up to 42 days. The RPC average compressive strength at the age of 28 and 42 days were 120.65 MPa and 117.84 MPa, respectively.

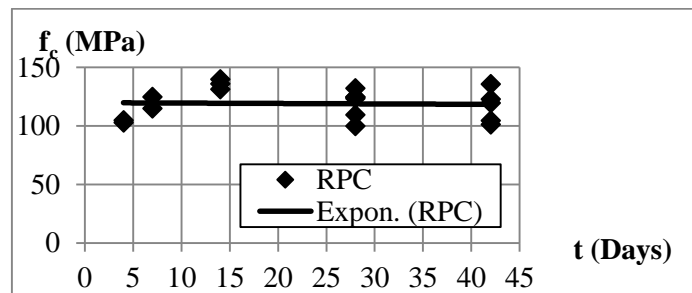


**Figure 6.** Relationship of Age with Compressive Strength of RPC.

### 1.2. Comparison of BCS-RPC Prototype and Finite Element Model Hysteretic Curves

The results of the BCS-RPC-31.72 prototype experiment were compared with the BCS-RPC-31.72 model. Figure 7 shows that the hysteretic curve of BCS-RPC-31.72 model was relatively close to the hysteretic curve of BCS-RPC-31.72 prototype with almost the same deflections ( $\delta$ ) and loads ( $F$ ). Figure 8 shows that the gradient of the backbone curve of the BCS-RPC-31.72 model was close to one of the BCS-RPC-31.72 prototype.

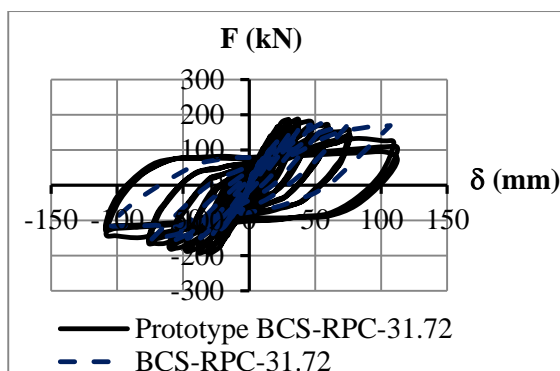


**Figure 7.** Hysteretic Curves of Prototype and Model of BCS-RPC-31.72.

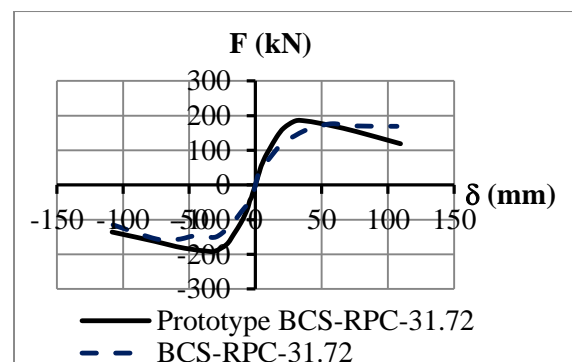


**Figure 8.** Backbone Curves of Prototype and Model of BCS-RPC-31.72.

### 1.3. Behavior of BCS-RPC and BCS-NC Models

Modeling of BCS-RPC and BCS-NC generated hysteretic curves (load-deflection relation) as shown in figure 9. The BCS-RPC-21.39 model achieved drift ratio of 5.00% under push loading (positive) and 3.50% under pull loading (negative). The BCS-RPC-31.72 model achieved drift ratio of 5.00% both under push and pull loadings. Under push loading, the BCS-NC-21.09 and BCS-NC-32.02 models achieved drift ratio of 3.50% and 5.00%, respectively. While under pull loading, the BCS-NC-21.09 and BCS-NC-32.02 models achieved the same drift ratio of 3.50%. All BCS-RPC models had higher initial stiffnesses than all BCS-NC models as shown in figure 10. This was because the RPC has a higher compressive strength than NC at the same strain. The values of maximum drift ratio, maximum deformation, and yield deformation are shown in table 2.

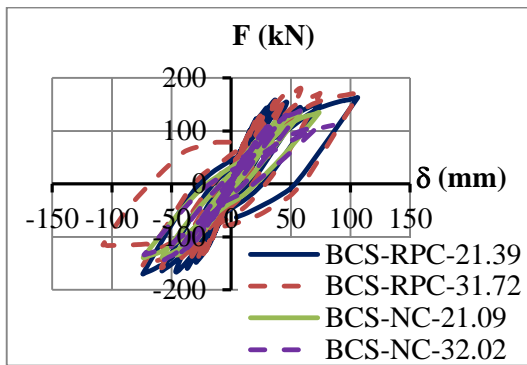


**Figure 9.** Hysteretic Curves of BCS-RPC and BCS-NC Models

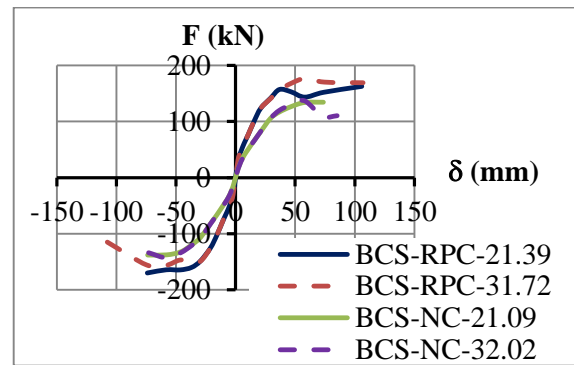


**Figure 10.** Backbone Curves of BCS-RPC and BCS-NC Models.

**Table 2.** Achieved Drift Ratio, Maximum Deformation, and Yield Deformation.

Model	Achieved Drift Ratio		Maximum Deformation		Yield Deformation	
	(+)	(-)	$\delta_{max (+)}$	$\delta_{max (-)}$	$\delta_y (+)$	$\delta_y (-)$
	(+)	(-)	(+)	(-)	(+)	(-)
	(%)	(%)	(mm)	(mm)	(mm)	(mm)
BCS-RPC-21.39	5.00	3.50	105.91	-74.02	15.80	-15.81
BCS-RPC-31.72	5.00	5.00	106.91	-107.48	15.80	-15.81
BCS-NC-21.09	3.50	3.50	73.67	-73.70	15.76	-15.77
BCS-NC-32.02	5.00	3.50	85.25	-73.08	15.76	-15.77

The stiffness degradation ( $K/K_y$ ) of all BCS-RPC and BCS-NC models were relatively similar since the drift ratio of 0.2% until the maximum achieved drift ratio of each model both under push and pull loading as shown in figure 11 and figure 12, respectively. All BCS-RPC models showed lower strength degradation ( $F/F_y$ ) than all BCS-NC models under push and pull loading as shown in figure 13 and figure 14, respectively. It indicates that all BCS-RPC models had more stable strength than all BCS-NC models. The strength degradation of BCS-RPC-21.39 model decreased at drift ratio of 2.75% and increased at drift ratio of 3.50%. The BCS-RPC-31.72 and BCS-RPC-21.39 models showed relatively equal strength degradation up to drift ratio of 1.75%. The BCS-NC-21.09 and BCS-NC-32.02 models had relatively same strength degradation under push and pull loading up to the drift ratio of 2.75%. The BCS-NC-32.02 model had decreased strength degradation at the drift ratio of 3.50% under push loading.

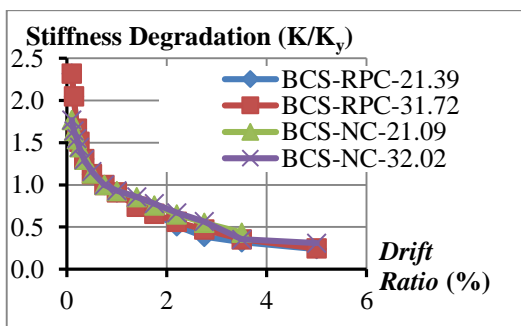


**Figure 11.** Stiffness Degradation under Push Loading.

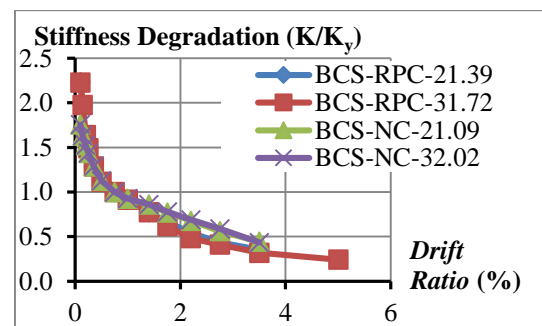


**Figure 12.** Stiffness Degradation under Pull Loading.

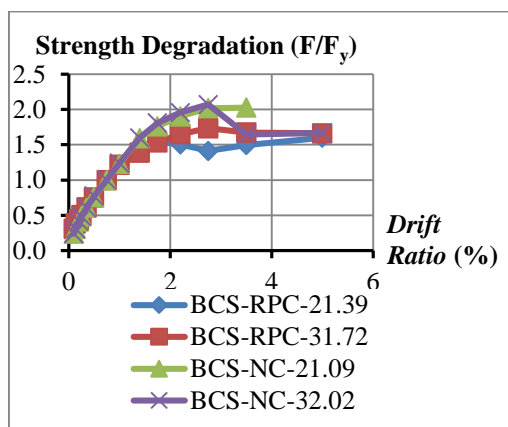


**Figure 13.** Strength Degradation under Push Loading.

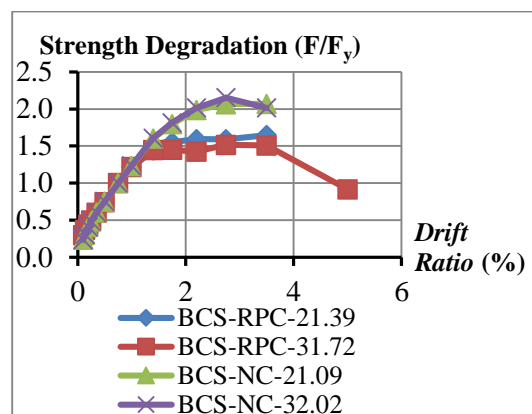


**Figure 14.** Strength Degradation under Pull Loading.

Table 3 shows the values of ductility ( $\mu$ ) and energy dissipation ( $E_d$ ) of all models. The achieved maximum drift ratio affected the ductility and energy dissipation of each model. Despite BCS-RPC-31.72 model had PPR over 25%, it developed the highest ductility than other models because it was able to achieve the drift ratio up to 5.00% under push and pull loadings. It indicates that the PPR of 31.72% still allows the model to behave ductile. Under push loading, the values of the next highest ductility achieved by the BCS-RPC-21.39, BCS-NC-32.02, and BCS-NC-21.09 models, respectively. While under pull loading, the values of the next highest ductility achieved by the BCS-RPC-21.39, BCS-NC-21.09, and BCS-NC-32.02 models, respectively.

**Table 3.** Ductility of BCS-RPC dan BCS-NC Models.

Model	Ductility		Ductility/Maximum Ductility		Energy Dissipation	
	$\mu$ (+)	$\mu$ (-)	$\mu/\mu_{\max}$ (+)	$\mu/\mu_{\max}$ (-)	$E_d$	$E_d/E_{d\max}$
			(%)	(%)	(kN.m)	(%)
BCS-RPC-21.39	6.70	4.68	1.00	0.69	23.57	76.91
BCS-RPC-31.72	6.77	6.80	1.01	1.00	30.64	100.00
BCS-NC-21.09	4.68	4.67	0.70	0.69	11.10	36.24
BCS-NC-32.02	5.41	4.63	0.81	0.68	9.98	32.58

The highest energy dissipation was achieved by the BCS-RPC-31.72 model because it had a higher nominal moment than the BCS-RPC-21.39 model, that allowed it to resist loads better and achieved the drift ratio up to 5.00% under the push and pull loadings. The BCS-NC-21.09 and BCS-NC-32.02 models only had energy dissipation by 36.24% and 32.58% of the energy dissipation of BCS-RPC-31.72 model, despite had nominal moment nearly equal to or greater than all BCS-RPC models. This was due in high drift ratio loadings, the NC ability was lower than RPC's in resisting lateral loads, that caused all BCS-NC models had a lower strength than all BCS-RPC models.

### Conclusion

From the finite element method modeling, some conclusions can be written as follows:

- The modeling of partial prestressed beam-column subassemblages made of Reactive Powder Concrete (RPC) material was able to provide information of performance of prestressed beam-column subassemblage prototypes as proven by the hysteretic curve shape of the model was relatively close to the hysteretic curve of prototype test results. Then the model can be used as a platform for modeling the beam-column subassemblages made of Normal Concrete (NC).

- Analysis of all of beam-columns subassemblage models made of RPC and NC showed that all BCS-RPC models had better performance in terms of strength, stiffness, ductility, and energy dissipation than all BCS-NC models.
- The BCS-RPC-31.72 model that had PPR over 25% exhibited ductile behavior up to drift ratio of 5.00% under push and pull loadings and dissipate energy better than BCS-RPC-21.39 model which had PPR less than 25%.

### Acknowledgment

The primary financial support for the research program was provided by P.T. Wijaya Karya Beton, Indonesia under joint research with the Faculty of Civil and Environment Engineering, Bandung Institute of Technology on contract number KU.09.09/OA.WB.191/2014 and 167/I1.C09/DN/2014.

### References

- [1] Richard P and Cheyrezy M, Composition of Reactive Powder Concrete, *Cement and Concrete Research*, Vol. 25 No.7 (1995) 1501 – 1511.
- [2] Thompson K J dan Park R, Ductility of Prestressed and Partially Prestressed Concrete Beam Sections, *Precast/Prestressed Concrete Institute Journal*. (March-April 1980) 46-70.
- [3] National Standardization Board, SNI 03-2847-2013 Procedure of Calculation of Concrete Structures for Buildings, Jakarta, Indonesia. (2013)
- [4] Gowripalan N, Watters R, Gilbert R I, and Cavill B, Reactive Powder Concrete for Precast Structural Concrete-Research and Development in Australia, *21st Biennial Conference of The Concrete Institut of Australia*, Brisbane, Australia (2003) 99-108.
- [5] Graybeal B A, Compressive Behavior of Ultra-High-Performance Fibre-Reinforced Concrete, *ACI Materials Journal*, Vol. 104, No. 2. (March-April 2007)
- [6] Menefy L, Investigation of Reactive Powder Concrete and Its Damping Characteristics When Utilized in Beam Elements. *Thesis of Doctor Philosophy*, Griffith School of Engineering, Griffith University, Gold Coast Campus, Australia. (2007)
- [7] Naibaho P R, Budiono B, Surono A, Pane I, Experimental Study of Reinforcement Addition on Exterior Beam-Column Connections Using Reactive Powder Under Cyclic Load, *Proceedings of the National Conference in Graduate Program of Civil Engineering*, Bandung Institute of Technology. (2014)
- [8] ACI Committee, Acceptance Criteria for Moment Frames Based on Structural Testing and Commentary, ACI 374.1-05, Farmington Hills, USA. (2005)